Journal of Manufacturing Processes 32 (2018) 327–336

Contents lists available at ScienceDirect

Journal of Manufacturing Processes

journal homepage: www.elsevier.com/locate/manpro

Modeling of cavitating flow induced by an ultrasonic horn above a solid target with a microhole

Navid Dabir-Moghaddam[a], Hanyu Song[b], Benxin Wu[b,*]

[a] Department of Mechanical, Materials and Aerospace Engineering, Illinois Institute of Technology, Chicago, IL, 60616, United States
[b] School of Mechanical Engineering, Purdue University, West Lafayette, IN, 47907, United States

ARTICLE INFO

Article history:
Received 17 February 2017
Received in revised form
23 November 2017
Accepted 7 February 2018

Keywords:
Ultrasonic cavitation
Ultrasound
Ultrasonic horn

ABSTRACT

Ultrasonic cavitation may be involved in many manufacturing-related applications, such as ultrasonic cleaning, ultrasonic cavitation peening, and ultrasound-assisted water-confined laser micromachining (UWLM). However, the previous physics-based modeling work has been very limited for cavitating flow induced by an ultrasonic horn near a solid target with a microhole. Such modeling work is reported in this paper, where two-dimensional compressible fluid mechanics equations, together with an equation governing the vapor-volume fraction evolution, are solved numerically. The model prediction shows reasonable consistency with experimental results in the literature for cavitating flow induced by an ultrasonic horn in water relatively far from a solid wall. Then the model is used to study the cavitating flow induced by a horn placed near a solid wall with a microhole. Under the studied conditions, the model calculations show that the horn-induced peak pressure magnitude at the microhole center decreases as the hole becomes deeper. On the other hand, the horn-induced temporal peak pressure at the hole bottom surface is spatially relatively uniform in the r (radial) direction, while the peak pressure on a solid surface without the hole decreases quickly with r. However, the peak pressure induced on the hole sidewall is not spatially uniform, and the largest peak pressure on the sidewall occurs at the hole bottom. The model may help future fundamental research work on ultrasonic horn-induced cavitating flow near a solid wall with a microhole, and may also provide a useful guiding tool for related manufacturing applications.

1. Introduction

Ultrasonic waves in water, such as those induced by an ultrasonically vibrating horn immersed in water, can induce cavitation when the waves are sufficiently strong [1–3]. Clouds of bubbles may be generated, and the growth and collapse of the bubbles may induce very high pressures [4]. Ultrasonic cavitation may be involved in many manufacturing-related applications, such as ultrasonic cleaning [5], ultrasonic cavitation peening [4], and ultrasound-assisted water-confined laser micromachining (UWLM) [6].

Microholes are often needed in numerous fields (e.g., the cooling holes in gas turbine engines, the fuel injection holes in engines, and other microholes that may be needed in electronic and biomedical devices) [7,8]. When the aforementioned ultrasonic cleaning, ultrasonic cavitation peeing or UWLM process is used to process or produce microholes, an essential process that may often be involved is the cavitating flow induced by an ultrasonic horn placed near a solid target surface with microhole(s). A physics-based model for such cavitating flow is highly desirable to improve the fundamental understanding of the process, because a full process understanding is difficult to achieve through experimental measurements alone. The model may also provide a helpful guiding tool for the process design, analysis and optimization in relevant applications.

Previous research work on the modeling of cavitating flow induced by an ultrasonic horn has been reported in the literature (e.g., in [9–15]. However, previously reported work in the literature has been very limited on the modeling of cavitating flow induced by an ultrasonic horn near a solid target *with a microhole*. Ref. [9] reports numerical modeling of cavitation induced by an ultrasonic horn that is a little far from a bottom wall. In Ref. [10], a computational modeling study has been performed on the cavitating flow induced by a horn tip that is close to the surface of a specimen. Ref. [11] reports CFD study of the flow pattern induced by a horn that vibrates ultrasonically, and in the model the horn tip displacement is a function of both time and the radial position. Ref. [12] reports

* Corresponding author at: School of Mechanical Engineering, Purdue University, 585 Purdue Mall, West Lafayette, IN, 47907, United States.
E-mail address: wu65@purdue.edu (B. Wu).

https://doi.org/10.1016/j.jmapro.2018.02.010
1526-6125/

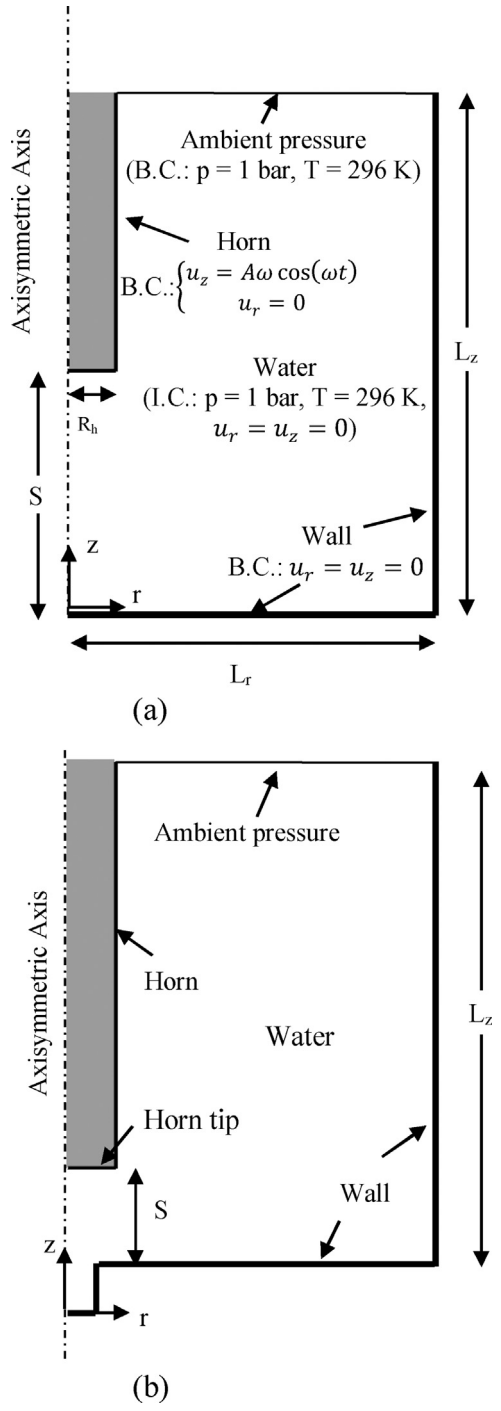

Fig. 1. Schematic diagram of the model for cavitating flow induced by an ultrasonic horn above a solid wall, (a) without, and (b) with a microhole (I.C.: initial conditions; B.C.: boundary conditions).

numerical modeling study of ultrasonic horn-induced cavitation in liquid aluminum, where a high-order method has been used in the spatial and temporal discretization of the wave equation. Ref. [13] reports simulations on the flow through a rectangular duct equipped with an ultrasonic horn on the bottom side of the duct. Ref. [14] reports computational modeling work on low-frequency ultrasonic horn reactors. Ref. [15] reports numerical simulation on the cavitating flow induced by an ultrasonic horn that is placed closely above a sample for vapor structure analysis and the erosion-sensitive area assessment. However, Refs. [9–15] did not perform modeling studies of cavitating flow induced by an ultrasonic horn near a solid surface *with a microhole*.

In this paper, a physics-based computational modeling study has been performed on the cavitating flow induced by an ultrasonically vibrating horn near a solid target surface with a microhole. In the model, 2D axisymmetric compressible fluid flow equations of mass, momentum and energy conservations have been solved for the fluid medium (which is assumed to be a potential mixture of water liquid and water vapor in bubbles) together with an equation that governs the vapor-volume fraction evolution based on the Schnerr-Sauer cavitation model [16–22]. Experimental results in the literature are used to test the model. Then the model is applied to study the cavitating flow induced by an ultrasonic horn near a solid surface with a microhole of different depths.

2. The model

Fig. 1 shows the schematic diagram for the model computational domain, and some major related initial conditions (I.C.) and boundary conditions (B.C.). At t = 0, it is assumed that the domain is filled with stationary liquid water at T = 296 K and P = 1 bar. At the upper boundary of the domain, a boundary condition of P = 1 bar and T = 296 K has been assumed. At r = 0, the axisymmetric boundary condition is applied. For all the other domain boundaries (including the horn side and bottom walls), the no-slip (for the velocities) and adiabatic boundary conditions are assumed. The ultrasonic horn is assumed to be rigid. At t = 0, the horn bottom has an initial distance of S from the domain bottom wall, and starts vibrating at 20 kHz with a certain peak-to-peak amplitude. The horn tip has a radius of R_h. As a comparison, model calculations are performed for the situation where a microhole exists (Fig. 1b) and the situation where a microhole does not exit (Fig. 1a) at the domain bottom wall. When a microhole exists, z = 0 is defined at the hole bottom, and when the hole does not exist, z = 0 is defined at the surface of the domain bottom wall. In the model calculations, the computational domain size in r and z direction is L_r and L_z, respectively.

The fluid in the domain is assumed to be a potential mixture of liquid water and water vapor bubbles, which is compressible. The initial vapor volume fraction is assumed to be 0. The evolution of the fluid is governed by mass, momentum and energy conservation equations in the two-dimensional (2D) axisymmetric form (Eqs. (1)–(3)) and an equation for the vapor volume fraction evolution (Eq. (4) [16–20]:

$$\frac{\partial \vec{A}}{\partial t} + \frac{1}{r}\frac{\partial \vec{B}}{\partial r} + \frac{\partial \vec{C}}{\partial z} = \vec{D} \tag{1}$$

$$\vec{A} = \begin{bmatrix} \rho \\ \rho u_r \\ \rho u_z \\ E + 0.5\rho u^2 \end{bmatrix}, \vec{B} = \begin{bmatrix} \rho r u_r \\ \rho r u_r^2 \\ \rho r u_r u_z \\ r u_r \left(p + E + 0.5\rho u^2\right) \end{bmatrix},$$

$$\vec{C} = \begin{bmatrix} \rho u_z \\ \rho u_r u_z \\ \rho u_z^2 \\ u_z \left(p + E + 0.5\rho u^2\right) \end{bmatrix} \tag{2}$$

$$\vec{D} = \begin{bmatrix} 0 \\ \frac{\tau_{rr}}{r} + \frac{\partial \tau_{rr}}{\partial r} + \frac{\partial \tau_{zr}}{\partial z} - \frac{\tau_{\theta\theta}}{r} - \frac{\partial p}{\partial r} \\ \frac{\tau_{rz}}{r} + \frac{\partial \tau_{rz}}{\partial r} + \frac{\partial \tau_{zz}}{\partial z} - \frac{\partial p}{\partial z} \\ \frac{1}{r}\frac{\partial}{\partial r}\left(rk\frac{\partial T}{\partial r}\right) + \frac{\partial}{\partial z}\left(k\frac{\partial T}{\partial z}\right) + \nabla\cdot\left(\tau\cdot\vec{u}\right) + S_{E,c} \end{bmatrix} \tag{3}$$